BIOCHEMISTRY
including biophysical chemistry & molecular biology

Article

pubs.acs.org/biochemistry

Probing the Dynamics of a His73−Heme Alkaline Transition in a Destabilized Variant of Yeast Iso-1-cytochrome *c* with Conformationally Gated Electron Transfer Methods

Swati Bandi[†] and Bruce E. Bowler*

Department of Chemistry and Biochemistry and Center for Biomolecular Structure and Dynamics, The University of Montana, Missoula, Montana 59812, United States

Supporting Information

ABSTRACT: The alkaline transition of cytochrome *c* involves substitution of the Met80 heme ligand of the native state with a lysine ligand from a surface Ω-loop (residues 70 to 85). The standard mechanism for the alkaline transition involves a rapid deprotonation equilibrium followed by the conformational change. However, recent work implicates multiple ionization equilibria and stable intermediates. In previous work, we showed that the kinetics of formation of a His73−heme alkaline conformer of yeast iso-1-cytochrome *c* requires ionization of the histidine ligand (pK_{HL} ∼ 6.5). Furthermore, the forward and backward rate constants, k_f and k_b, respectively, for the conformational change are modulated by two auxiliary ionizations (pK_{H1} ∼ 5.5, and pK_{H2} ∼ 9). A possible candidate for pK_{H1} is His26, which has a strongly shifted pK_a in native cytochrome *c*. Here, we use the AcH73 iso-1-cytochrome *c* variant, which contains an H26N mutation, to test this hypothesis. pH jump experiments on the AcH73 variant show no change in k_{obs} for the His73−heme alkaline transition from pH 5 to 8, suggesting that pK_{H1} has disappeared. However, direct measurement of k_f and k_b using conformationally gated electron transfer methods shows that the pH independence of k_{obs} results from coincidental compensation between the decrease in k_b due to pK_{H1} and the increase in k_f due to pK_{HL}. Thus, His26 is not the source of pK_{H1}. The data also show that the H26N mutation enhances the dynamics of this conformational transition from pH 5 to 10, likely as a result of destabilization of the protein.

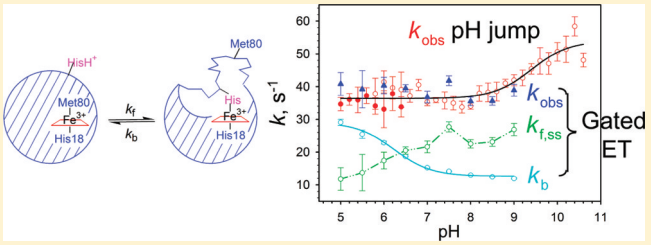

The alkaline conformational transition of cytochrome *c* (Cyt*c*) is a long-studied rearrangement of the structure of mitochondrial Cyt*c* that occurs at mildly alkaline pH.[1−3] Initial studies indicated a simple two-state conformational change with a kinetic mechanism involving a rapid deprotonation equilibrium followed by the conformational change.[4] The identity of the ionizable group that triggers this transition has been long debated.[1−3] More recent studies have shown that multiple ionizations are involved in this conformational transition[5−8] and that equilibrium intermediates form during the alkaline transition.[7−14] Thus, a conformational change that was viewed to be quite simple is indeed complex. In this work, we use a novel conformationally gated electron transfer method[15] to probe in detail the role of ionization of His26 in the mechanism of this conformational transition. We also investigate in more depth the effect of overall protein stability on the dynamics of this conformational change.[15]

For wild-type (WT) type *c* cytochromes, lysines in a surface Ω-loop that includes residues 70−85 replace the native-state axial heme ligand, Met80,[16−19] leading to a significant rearrangement of this Ω-loop.[20] For yeast iso-1-Cyt*c*, Lys73 and Lys79 replace Met80 in the alkaline state.[16,17] It has been suggested that alkaline conformers of Cyt*c* may be important in mediating the function of Cyt*c* in both electron transport[20−22] and apoptosis.[23,24] Thus, a more complete understanding of the alkaline transition may be important for understanding the biological functions of Cyt*c*.

Hydrogen-exchange (HX) experiments have shown that horse Cyt*c* and *Pseudomonas aeruginosa* cytochrome c_{551} are made up of substructures or foldons that unfold sequentially, from least to most stable.[25−28] Yeast iso-1-Cyt*c* is considerably less stable than horse Cyt*c*, yet the foldon structure appears to be preserved.[29] The dynamic range of foldon energies is, however, severely compressed in yeast iso-1-Cyt*c* relative to horse Cyt*c*.[29] Figure 1 shows the foldons of the horse protein mapped onto the structure of yeast iso-1-Cyt*c*. As defined by Englander and co-workers,[25,26] they are from least to most stable: Infrared (Ω-loop running from residue 40 to 57, colored gray), Red (Ω-loop running from residue 70 to 85), Yellow (short β-sheet, residues 36−39 and 58−61), Green (Ω-loop running from residue 20 to 35 and the sixties helix), and Blue (N- and C-terminal helices). A nuclear magnetic resonance structure of the Lys73−heme alkaline conformer,[20] HX studies of horse Cyt*c*,[19,30] and thermodynamic studies of yeast iso-1-Cyt*c*[31,32] are consistent with disruption of the Ω-loop corresponding to the Red foldon during the alkaline transition

Received: July 13, 2011
Revised: October 22, 2011
Published: October 25, 2011

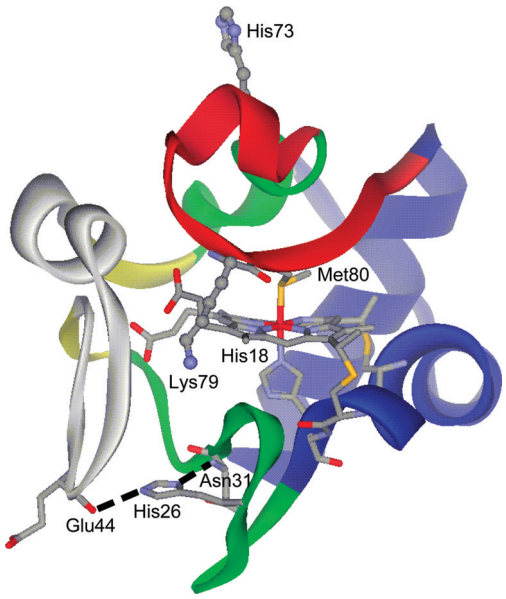

Figure 1. Iso-1-Cyt*c* showing the side chains of His73 (K73H mutation added to Protein Data Bank entry 2ycc using the mutate function of HyperChem) and Lys79 as ball and stick models colored by element. The heme cofactor, heme ligands Met80 and His18, and Cys14 and Cys17, which covalently attach the heme to the polypeptide chain, are shown as stick models colored by element. The side chain of His26 is shown hydrogen-bonded to the carbonyl of Glu44 and the amide NH group of Asn31. The substructures (foldons) of Cyt*c* are color-coded as described in the text.

(Figure 1). However, kinetic studies indicate that transient unfolding of the least stable Infrared substructure is required during the alkaline transition.[30]

We have recently reported that the dynamics of the alkaline transition of iso-1-Cyt*c* near neutral pH are strongly affected by mutation of His26 to Asn (H26N).[15] The side chain of His26 forms hydrogen bonds that bridge two of the foldons of Cyt*c* (Figure 1). His26 also has a strong cooperative effect on the stability of iso-1-Cyt*c*,[33,34] with the H26N mutation strongly destabilizing iso-1-Cyt*c*.[15,35,36] This destabilization is consistent with the observation that protonation of His26 destabilizes the Ω-loop that runs from residue 20 to 36 (part of the Green foldon in Figure 1) at acidic pH.[27] The Infrared (gray in Figure 1) foldon is also destabilized at lower pH, with the destabilization attributable to both protonation of His26 and heme propionate 7 (HP-7, the inner heme propionate).[26]

In previous work, we have used K73H and K73H/K79A variants of iso-1-Cyt*c* to study the alkaline transition.[5,6] These variants replace Lys73 with histidine, leading to the formation of a His73−heme alkaline conformer in lieu of the normal Lys73−heme alkaline conformer (even though the His73−heme conformer forms near neutral pH, we call it the alkaline conformer because of its correspondence to the naturally occurring Lys73−heme alkaline conformer). The thermodynamics and kinetics of the interconversion between the native conformer and the His73−heme alkaline conformer are consistent with deprotonation of His73 being the primary ionization that promotes the alkaline transition.[5,6] Two auxiliary ionizations, one with a pK_a of ∼5.5 and the other with a pK_a of ∼9, modulate the magnitude of the forward and backward rate constants.[5,6] HP-7 and His26 both have unusual pK_a values shifted below 4.5 by their environments in the native state.[37−40] Because both His26 and a heme propionate have been implicated in affecting the stability of the Infrared and Red foldons, either is a likely candidate for the auxiliary ionization with a pK_a of ∼5.5.

To probe the effect of His26 on the mechanism of the alkaline transition, we use the AcH73 variant of iso-1-Cyt*c*.[15,36] This variant was developed to simplify heme ligation equilibria in the fully denatured state of iso-1-Cyt*c*,[35,36] permitting more careful control of the effect of the denatured state on global stability. In addition to the K73H mutation present in the K73H variant, this variant contains the following mutations: T(−5)S, K(−2)L (permits N-terminal acetylation in vivo preventing binding of the N-terminal amino group to the heme in the denatured state,[36,41] hence the Ac in the variant name; note horse numbering is used, thus the first five residues of the yeast protein are numbered −5 to −1), and H26N, H33N, and H39Q (that prevent histidine misligation in the denatured state[36]). Of these five mutations, only the H26N mutation significantly affects the stability of iso-1-Cyt*c*,[33−36] and thus, the other mutations can be viewed as spectator mutations. Thus, the H26N mutation is expected to dominate any differences between the K73H and AcH73 variants of iso-1-Cyt*c*. If His26 is responsible for the ionization near pH 5.5, which affects the kinetics of the His73−heme alkaline transition of the K73H variant, this ionization should be eliminated in the kinetics of the His73−heme alkaline transition of the AcH73 variant. The AcH73 variant is considerably less stable than the K73H variant we have studied previously.[15,36] Thus, kinetic studies of the His73−heme alkaline transition of AcH73 iso-1-Cyt*c* also allow evaluation of the effect of global stability on the dynamics of the alkaline transition.

EXPERIMENTAL PROCEDURES

Isolation, Purification, and Characterization of the AcH73 Variant of Iso-1-Cyt*c*. The AcH73 variant[36] was isolated and purified from *Saccharomyces cerevisiae* as described previously.[34,42] The purification of the AcH73 protein by cation-exchange high-performance liquid chromatography gave one main peak. The main peak was collected and concentrated using Centricon and Centriprep concentrators (10000 molecular weight cutoff, Millipore), exchanged into 50 mM sodium phosphate buffer (pH 7), and concentrated to a final volume of ∼500 μL. Mass spectrometry was conducted using an Applied BioSystems Voyager-DE Pro Biospectrometry Workstation. The main peak gave m/z 12672 ± 3 (expected mass, 12675.21 Da). All experiments were conducted with this material.

Oxidation of Protein. Protein was oxidized with $K_3[Fe(CN)_6]$ and separated from oxidizing agent by Sephadex G25 chromatography using running buffer appropriate to the experiment. The concentration and degree of oxidation of the protein were determined as described previously.[36]

pH Titration Experiments. The alkaline conformational transition caused by His73 was monitored as a function of pH at 0, 0.1, 0.2, and 0.3 M guanidine hydrochloride (gdnHCl) using the 695 nm absorbance band (Beckman DU 800 spectrophotometer). The experiment was conducted at 22 ± 1 °C. The initial sample was made by mixing 500 μL of ∼400 μM protein in 200 mM NaCl or 20 mM MES in 200 mM NaCl (2× protein in 2× buffer) with 500 μL of doubly deionized water (ddH_2O). For 0.1, 0.2, and 0.3 M gdnHCl samples, back-titrations were also conducted. The solution was mixed with a 1000 μL pipetman, and the pH was adjusted to either 4.5 or 5.7 by addition of 3 M HCl and an equal volume of 2× protein in

2× buffer. The pH titrations at 0 and 0.1 M gdnHCl were initiated at pH 5.7 as the AcH73 variant tended to aggregate at lower pH. The pH was measured with an Accumet AB15 pH meter (Fisher Scientific) using an Accumet semimicro calomel pH probe (Fisher Scientific, catalog no. 13-620-293). The experiment was conducted as described previously.[6,43] The absorbance at 750 nm was used as the background wavelength to control for baseline drift, using the relationship $A_{695corr} = A_{695} - A_{750}$. The molar extinction coefficient at each pH was calculated for all pH titrations as described previously,[43] with the protein concentration determined from the absorbance at pH 5 at 570 and 580 nm using oxidized-state extinction coefficients of 5.2 and 3.5 mM^{-1} cm^{-1}, respectively.[44] The molar extinction coefficient at 695 nm versus pH data were fitted to eq 1.

$$\varepsilon_{695corr} = \frac{\varepsilon_N + \varepsilon_{alk}\left(\frac{10^{-pK_{C1}}}{1+10^{pK_{a,1}-pH}} + \frac{10^{-pK_{C2}}}{1+10^{pK_{a,2}-pH}}\right)}{1 + \frac{10^{-pK_{C1}}}{1+10^{pK_{a,1}-pH}} + \frac{10^{-pK_{C2}}}{1+10^{pK_{a,2}-pH}}} \quad (1)$$

where $\varepsilon_{695corr}$ is the corrected molar extinction coefficient at 695 nm during the alkaline transition, ε_N is the corrected molar extinction coefficient at 695 nm of the Met80-bound native state, and ε_{alk} is the corrected molar extinction coefficient at 695 nm of the alkaline state. In fitting the data for the AcH73 variant, we have constrained ε_{alk} to equal $\varepsilon_N - 0.53$ mM^{-1} cm^{-1}, as observed in pH titration studies with the K73H variant.[31] K_C is the equilibrium constant associated with the replacement of Met80 with an alternative ligand, and K_a is the triggering deprotonation equilibrium. For pK_{C1}, the alternate ligand is His73, and for pK_{C2}, the alternate ligand is Lys79. $pK_{a,1}$ and $pK_{a,2}$ are the pK_a values of the triggering group that is deprotonated when the His73 and Lys79 side chains replace Met80, respectively. $pK_{a,2}$ was constrained to 10.8 on the basis of previous data[17] to facilitate fits.

pH Jump Stopped-Flow Experiments. All pH jump experiments were conducted at 25 °C, and data were collected at 405 nm on 5 and 50 s time scales with an Applied Photophysics SX20 stopped-flow spectrophotometer as described previously.[43] For upward pH jumps, an initial pH of 5 in unbuffered 0.1 M NaCl containing ~20 μM protein was used, because the population of the native state of the AcH73 variant is maximal near this pH. Data were collected at final pH values from 5.8 to 11.2. Final pH values were achieved by mixing the initial solution with an equal volume of 20 mM buffer in 0.1 M NaCl to produce a final solution of 10 μM protein in 10 mM buffer at the desired pH containing 0.1 M NaCl. For downward pH jumps, the initial pH was set to 7.8 (to focus on the kinetics due to the His73–heme conformer, which is dominant under equilibrium conditions at this pH[31]), and data were collected for final pH values of 5–6.4. Buffers used to control the final pH after stopped-flow mixing were acetic acid (pH 5–5.4), MES (pH 5.6–6.6), NaH_2PO_4 (pH 6.8–7.6), Tris (pH 7.8–8.8), H_3BO_3 (pH 9–10), and CAPS (pH 10–11.2) as in our previous work[5,6,43,45] and in other studies of the alkaline transition of iso-1-Cytc.[17] Each set of upward pH jump data was fit to a single- or double-exponential rise to maximum equations. Data for downward pH jumps were fit to single- or double-exponential decay equations, as appropriate. The k_{obs} (eq 2) and amplitude (eq 3) data as a function of pH for the fast and slow phases were fit to the usual mechanism for the alkaline conformational transition involving a rapid deprotonation equilibrium followed by a reversible conformational change.[4]

$$k_{obs} = k_b + k_f; \quad k_f = k_f'\left(\frac{1}{1+10^{pK_H-pH}}\right) \quad (2)$$

$$\Delta A_{405} = \Delta A_{405t}\left[\frac{1}{1+\frac{k_b}{k_f'}(1+10^{pK_H-pH})}\right] \quad (3)$$

where pK_H is the acid dissociation constant for the ionizable group triggering the conformational change, k_f and k_b are the forward and backward rate constants, respectively, for the conformational change, k_f' is the limiting value of k_f at high pH (trigger group fully deprotonated), ΔA_{405} is the change in amplitude at 405 nm, and ΔA_{405t} is the limiting change in amplitude at high pH.

Electron Transfer Experiments by the Stopped-Flow Method. Experiments were conducted using hexaammineruthenium(II) chloride (a_6Ru^{2+}) with an Applied Photophysics SX20 stopped-flow spectrophotometer, as described previously.[43] The stopped-flow assembly was made anaerobic by soaking the syringe assembly in 0.1 M sodium dithionite prepared in 0.1 M dibasic sodium phosphate (not pH-adjusted) overnight followed by soaking for 2–3 h in fresh solution on the day of the experiment.[46] The syringe assembly was then thoroughly washed with argon-purged 10 mM buffer prepared in 0.1 M NaCl. The 10 mM buffers used for these experiments were acetic acid (pH 5 and 5.5), MES (pH 6 and 6.5), NaH_2PO_4 (pH 7 and 7.5), Tris (pH 8 and 8.5), and H_3BO_3 (pH 9) to be coincident with the buffers used to achieve the final pH values after mixing in the pH jump stopped-flow experiments. The protein concentration after stopped-flow mixing with a_6Ru^{2+} was ~5 μM. Experiments were conducted at six different concentrations of a_6Ru^{2+}: 0.625, 1.25, 2.5, 5, 10, and 20 mM.

To determine the actual a_6Ru^{2+} concentration, the electronic absorption spectrum (250–500 nm) was acquired for a_6Ru^{2+} prepared in the argon-purged buffer before and after the experiment. Concentrations calculated from absorbance at 390 nm (ε_{390} = 35 M^{-1} cm^{-1}) and 400 nm (ε_{400} = 30 M^{-1} cm^{-1}) were averaged, yielding the concentration of a_6Ru^{2+}.[47,48] Direct concentration measurements turned out to be a critical factor in obtaining reproducible plots of rate constants for Cytc reduction versus a_6Ru^{2+} concentration.

Reduction of the heme after stopped-flow mixing of the AcH73 variant with a_6Ru^{2+} was monitored at 550 nm. At each concentration of a_6Ru^{2+}, five kinetic traces were collected. For all traces, 5000 points were collected logarithmically on a 50 s time scale. Analysis of the data was conducted using the curve fitting program SigmaPlot (version 7.0). The data were fit to a quadruple-exponential rise to maximum equation. At each pH, data acquired in the presence of ~1 mM a_6Ru^{2+} were fit by numerical methods using Pro-Kineticist (version 1, Applied Photophysics) to directly extract rate constants for conformational gating. Details of fitting procedures with Pro-Kineticist are provided in the Supporting Information.

RESULTS

Free Energy Landscape of His73-Containing Variants of Iso-1-Cytc. When Lys73 is replaced with histidine, the alkaline conformational transition is shifted to lower pH because of the lower intrinsic pK_a of histidine compared to that of lysine.[3] Histidine−heme ligation, unlike lysine−heme ligation, is unable to drive the alkaline conformational transition to completion. Thus, near pH 7.5, where His73 approaches full deprotonation, the native Met80−heme and alkaline His73−heme conformers are approximately equally populated and produce a two-well free energy surface (Figure 2). In previous work,[15,36] we have shown that the H26N mutation significantly destabilizes the AcH73 variant toward global unfolding by gdnHCl relative to the K73H variant that does not contain this mutation. The overall stability of the AcH73 variant is decreased to approximately half of that of K73H iso-1-Cytc. An H26V mutation also destabilizes rat Cytc.[49] The destabilization presumably results from disruption of a bridging hydrogen bond between two surface Ω-loops of Cytc mediated by the side chain of His26 (Figure 1).[50] Loss of this interaction also destabilizes the native state (Met80−heme ligation) relative to the His73−heme alkaline conformer (Figure 2). Kinetic studies also showed that the activation barrier at pH 7.5 between the native and His73−heme alkaline conformers is reduced in the less stable AcH73 variant relative to the more stable K73H variant.[15]

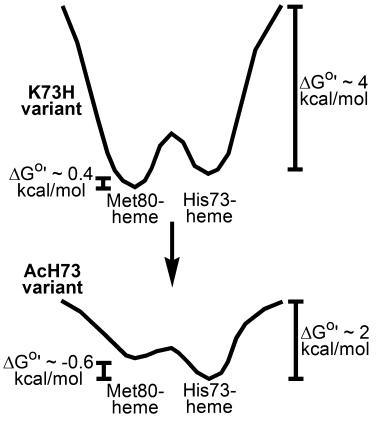

Figure 2. Free energy landscapes of the K73H and AcH73 variants near pH 7.5 showing the effects of the H26N mutation in the AcH73 variant on the relative stabilities of the native (Met80−heme), alkaline (His73−heme), and fully unfolded states of these two variants of iso-1-Cytc. The measured global stability is relative to the His73−heme alkaline conformer because nearly complete conversion to this form of the protein occurs prior to global unfolding by gdnHCl.[15,81]

There is some evidence that the N-terminal amino group can participate in the alkaline transition of horse cytochrome c,[19] but only in the absence of Lys79 and at pH values approaching 10. Because both the K73H variant (free N-terminal amino group) and AcH73 (acetylated N-terminal amino group) have Lys79, we do not expect that the difference in the availability of the N-terminal amino group contributes to any observed differences between the alkaline states of these variants in the pH range of our experiments.

Formation of Alkaline Conformers as a Function of pH and GdnHCl Concentration for AcH73 Iso-1-Cytc. The alkaline transition of variants of iso-1-Cytc with a K73H mutation is biphasic when monitored at 695 nm, a wavelength that is sensitive to the presence of heme−Met80 ligation.[1,51,52] The data can be fit to the thermodynamic model shown in Figure 3A (eq 1 in Experimental Procedures). In general, the p$K_{a,1}$ obtained from fitting data to this model is consistent with the acid dissociation equilibrium of a histidine.[6,31] In Figure 3A, for the sake of simplicity, we show p$K_{a,2}$ as resulting from the acid dissociation equilibrium of Lys79. While there are some data supporting this assignment,[53] it is not universally accepted.[1−3]

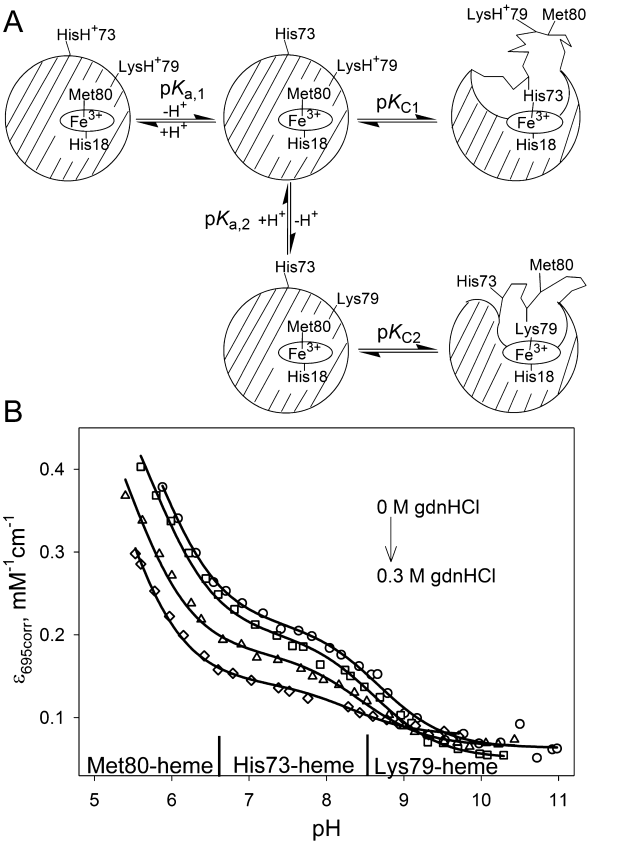

Figure 3. (A) Schematic representation of heme ligation equilibria as a function of pH for iso-1-Cytc variants containing a K73H mutation. The parameters p$K_{a,1}$, p$K_{a,2}$, pK_{C1}, and pK_{C2} are as defined for eq 1 in Experimental Procedures. (B) Plots of $\varepsilon_{695corr}$ vs pH for AcH73 iso-1-Cytc at different concentrations of gdnHCl. Data were collected at room temperature (22 ± 1 °C) in 0.1 M NaCl with 0 (○), 0.1 (□), 0.2 (△), and 0.3 (◇) M gdnHCl added. The solid curves are fits to the equilibrium scheme in part A using eq 1 in Experimental Procedures. The $\Delta\varepsilon_{695,corr}$ for the full transition was set to 0.53 mM^{-1} cm^{-1} as described in Experimental Procedures.

The conformational transition for the AcH73 variant was monitored as a function of pH and gdnHCl concentration using the 695 nm absorbance band. As with other variants with a K73H mutation, the AcH73 variant shows a biphasic pH titration curve at all gdnHCl concentrations, which was readily fitted to the thermodynamic model in Figure 3A using eq 1 (Experimental Procedures). The lower-pH phase of the transition does not completely eliminate the 695 nm band, and in the higher-pH phase of the transition, the 695 nm band is completely lost. Background subtraction was used to correct for light scattering because of a small amount of aggregation resulting from the low stability of the protein. Forward and backward pH titrations were performed with the same sample

at 0.1, 0.2, and 0.3 M gdnHCl (Figure S1 of the Supporting Information) to check the robustness of this method of analysis. Good agreement was observed between thermodynamic parameters from fits of forward and backward pH titration data to the thermodynamic model in Figure 3A (Table S1 of the Supporting Information), indicating that the effect of light scattering due to a small amount of aggregation is adequately removed by background subtraction. Thermodynamic parameters derived from the alkaline transition of the AcH73 variant at different concentrations of gdnHCl are summarized in Table 1.

Table 1. Thermodynamic Parameters from pH Titrations in 0.1 M NaCl at 22 ± 1 °C for the AcH73 Variant of Iso-1-Cyt*c*[a]

[gdnHCl] (M)	pK_{C1}	p$K_{a,1}$	pK_{C2}
0	−0.41 ± 0.02	6.16 ± 0.14	−2.58 ± 0.08
0.1	−0.53 ± 0.17	6.25 ± 0.22	−2.97 ± 0.44
0.2	−0.81 ± 0.15	6.24 ± 0.24	−3.40 ± 0.25
0.3	−0.91 ± 0.17	6.24 ± 0.21	−3.48 ± 0.23

[a]Parameters are the average and standard deviation from both forward and backward trials at 0.1−0.3 M gdnHCl and for three trials at 0 M gdnHCl from fits of the data to eq 1 in Experimental Procedures.

The value of p$K_{a,1}$ at all gdnHCl concentrations is between 6.1 and 6.3, consistent with a histidine, and is independent of gdnHCl concentration within error. The values of both pK_{C1} (His73−heme alkaline conformer) and pK_{C2} (Lys79−heme alkaline conformer) become progressively more negative (i.e., more favorable) as the gdnHCl concentration increases, as expected. If a linear free energy relationship is assumed for the gdnHCl concentration dependence of the alkaline transition (eq 4), m values of 2.4 ± 0.3 and 4.2 ± 0.8 kcal mol^{-1} M^{-1} (Figure S2 of the Supporting Information) are obtained for formation of the His73−heme and Lys79−heme alkaline conformers, respectively.

$$\Delta G_u = \Delta G_u^\circ(H_2O) - m[\text{gdnHCl}] \quad (4)$$

The m values indicate that the structural disruption for the higher-pH phase (Lys79−heme) is greater than that in the lower-pH phase (His73−heme) of the alkaline transition, as m values correlate with the amount of surface area exposed to solvent in a protein conformational transition.[54,55]

The m value we observe for the transition from the native conformer to the His73−heme alkaline conformer with the AcH73 variant is somewhat larger than the range of 1.4−1.7 kcal mol^{-1} M^{-1} that we have observed for this conformational transition with iso-1-Cyt*c* variants that contain His26.[6,31,32] Our previous studies have all been conducted with variants that are considerably more stable than the AcH73 variant. The larger m value suggests that the extent of structural disruption when the His73−heme alkaline conformer forms is larger for this less stable variant. The m value observed for the transition from the native conformer to the Lys79−heme alkaline conformer with the AcH73 variant is considerably larger than the range of 0.8−1.1 kcal mol^{-1} M^{-1} observed for this conformational transition for variants of iso-1-Cyt*c* that contain His26.[31,32] The magnitude of the m value is more similar to the value of 4−5 kcal mol^{-1} M^{-1} observed for global unfolding of iso-1-Cyt*c*.[35,56] Thus, it appears that formation of the Lys79−heme alkaline conformer in the unstable AcH73 variant may be coupled to global unfolding of the protein. Because the AcH73 variant is very unstable, the onset of alkaline denaturation likely occurs at a lower pH than for the more stable K73H variant.

pH Jump Kinetic Studies of the Alkaline Transition for the AcH73 Variant of Iso-1-Cyt*c*. In previous work, we have shown that the kinetics of the alkaline transition is considerably faster when His73 is the alkaline-state ligand[5,6] than when Lys73 or Lys79 acts as the alkaline-state ligand.[17,45] pH jump experiments for monitoring the kinetics of the alkaline transition of the AcH73 variant (representative kinetic data are shown in Figures S3−S6 of the Supporting Information) show two kinetic phases as expected (Figure 4): a fast phase

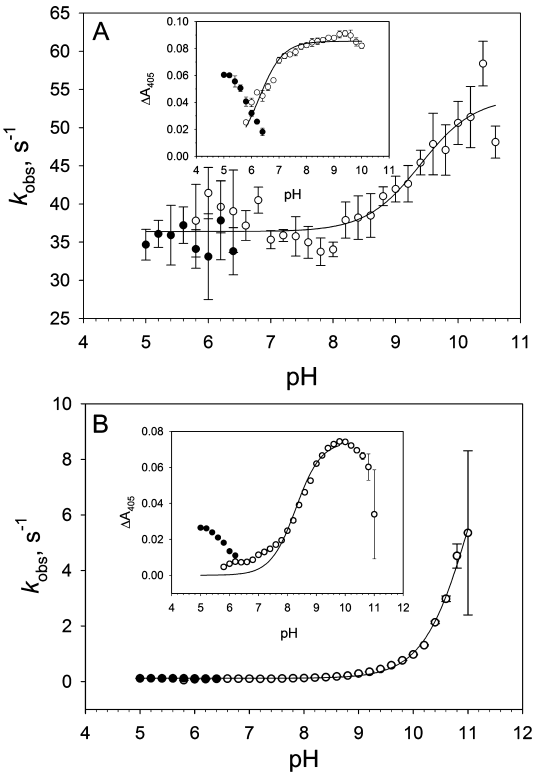

Figure 4. pH jump kinetic data for the alkaline transition of AcH73 iso-1-Cyt*c*. (A) Rate constants, k_{obs}, and amplitudes, ΔA_{405} (inset), as a function of pH for the fast phase from a 50 s time scale data set collected at 25 °C in 10 mM buffer containing 0.1 M NaCl. Empty circles depict data from upward pH jump experiments and filled circles data from downward pH jump experiments. (B) Rate constants, k_{obs}, and amplitudes, ΔA_{405} (inset), as a function of pH for the slow phase from 50 s data collected at 25 °C in 10 mM buffer containing 0.1 M NaCl. Empty circles depict data from upward pH jump experiments and filled circles data from downward pH jump experiments. In both panels A and B, the solid curve for k_{obs} vs pH is a fit to eq 2 in Experimental Procedures. In both insets, the solid curve for ΔA_{405} vs pH is a fit for upward pH jumps to eq 3 in Experimental Procedures. Parameters from these fits are listed in Table 2. Rate constants and amplitudes are listed in Tables S2−S7 of the Supporting Information.

(20−30 ms time scale) attributable to the His73−heme alkaline conformer and a slow phase (0.2−20 s time scale) attributable to the Lys79−heme alkaline conformer. The amplitude of the fast phase increases from pH 5.8 to 8 (inset, Figure 4A), as expected for the His73−heme alkaline conformer based on equilibrium pH titrations (Figure 3). Similarly, the amplitude for the slow phase (inset, Figure 4B) increases from pH 8 to 10, as expected for formation of a Lys79−heme alkaline conformer based on equilibrium pH titrations (Figure 3).

dx.doi.org/10.1021/bi201082h | *Biochemistry* 2011, 50, 10027−10040

The rate constants and amplitudes as a function of pH for both the fast and slow phases appear to be consistent with the standard mechanism for the alkaline conformational transition of Cyt*c*, which involves rapid deprotonation of a trigger group followed by the conformational change.[4] Parameters from fits of the fast phase (His73−heme alkaline conformer) and slow phase (Lys79−heme alkaline conformer) k_{obs} and amplitude data in Figure 4 to this mechanism are listed in Table 2.

Table 2. Rate and Ionization Constants Associated with the Fast and Slow Phases of the Alkaline Transition of AcH73 Iso-1-Cyt*c* at 25 °C in 0.1 M NaCl

parameter	fast phase[a]	slow phase[b]
k_f' (s^{-1})	16.5 ± 1.8	∼12
k_b (s^{-1})	35.5 ± 0.7	0.12 ± 0.02
pK_H (k_{obs} data)	9.4 ± 0.2	∼11
pK_H (ΔA_{405})	6.45 ± 0.05	10.30 ± 0.04

[a]Parameters are the average and standard deviation from three sets of k_{obs} and amplitude vs pH data fit to eqs 2 and 3 (Experimental Procedures), respectively. Two data sets were collected on a 5 s time scale, and one data set was collected on a 50 s time scale. [b]Parameters are the average and standard deviation from the fits of k_{obs} and amplitude vs pH data from a 50 s time scale data set to eqs 2 and 3 (Experimental Procedures), respectively. Because the upper limit of k_{obs} is not well-defined for the slow phase, the values of k_f' and pK_H are indicated as approximate values.

For this simple mechanism, the pK_H values for the fast and slow phases can be different if the ionizable groups triggering the transition to the His73−heme conformer versus the Lys79−heme conformer are different. However, for each phase, the pK_H values obtained from the k_{obs} and amplitude data should be the same or similar. For the fast phase data, the pK_H values obtained from the k_{obs} versus the amplitude data are dramatically different. The fit to the k_{obs} data also yields a k_f' that is one-half the magnitude of k_b. However, the thermodynamic data in Table 1 (pK_{C1} = −0.41 at 0 M gdnHCl) indicate that k_f' should be approximately twice the magnitude of k_b. These results indicate that the standard model for the alkaline conformational transition is not an adequate model for the formation of the His73−heme alkaline conformer. The observation of two very different pK_H values for amplitude versus k_{obs} data suggests that more than one ionizable group is involved in the kinetic mechanism of the His73−heme conformational transition.

The fit of the slow phase k_{obs} versus pH data, which we attribute to the Lys79−heme alkaline conformer, to the standard kinetic model for the alkaline transition yields a pK_H for deprotonation of the trigger group of ∼11. The fit to the amplitude data for the slow phase data yields a lower pK_H than the rate constant data, as for the fast phase, although the difference is not as dramatic and there is uncertainty in the pK_H obtained from the k_{obs} versus pH data because k_{obs} has not reached a plateau at high pH. The amplitude versus pH data for the slow phase do not increase smoothly. This behavior may result from an overlap in k_{obs} for the Lys79−heme alkaline conformer at low pH with a proline isomerization phase associated with the His73−heme alkaline conformer. In previous studies of the K73H and K73H/K79A variants, we have observed that proline isomerization associated with the His73−heme alkaline conformer and the kinetics of the Lys79−heme alkaline transition occur on the same time scale at pH <8.[5,6] Thus, the pK_H obtained from the slow phase amplitude data may also be less reliable than the indicated error in Table 2. A range of values is observed for pK_H with alkaline conformers involving lysine−heme ligation. In some variants of iso-1-Cyt*c*, pK_H values as low as 9−9.5 are observed.[57] For iso-1-Cyt*c*, the pK_H for the Lys79−heme alkaline transition is 10.8, whereas the pK_H is 12 for the Lys73−heme alkaline transition.[17] The pK_H values we observe for the slow phase are reasonably consistent with the pK_H observed for the Lys79−heme alkaline conformer of iso-1-Cyt*c*.

Conformationally Gated Electron Transfer Measurements. Previously, we have shown that the kinetic mechanism of the His73−heme alkaline conformational transition is more complex than the standard mechanism for the alkaline conformational transition.[5,6] To explain the pH-dependent behavior of k_{obs} for the His73−heme alkaline transition of the K73H and K73H/K79A iso-1-Cyt*c* variants, it was necessary to invoke three ionizable groups (Figure 5).[5,6] In this model,

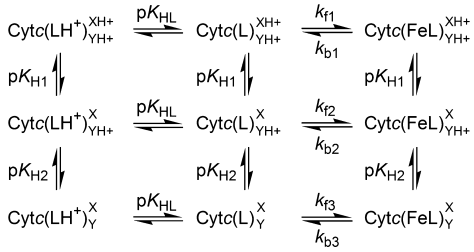

Figure 5. Kinetic mechanism for the alkaline conformational transition of Cyt*c* involving three ionizable groups.[5,6] The primary trigger is ionization of the ligand, represented by conversion of LH^+ to L with an ionization constant pK_{HL}. Ionization of the ligand unmasks a lone pair so that it may displace Met80 from the heme iron to form the alkaline conformer, FeL. Two other ionizable groups, XH+ and YH+, with ionization constants of pK_{H1} and pK_{H2}, respectively, modulated the barrier height for the alkaline conformational transition.

ionization of the ligand replacing Met80 (pK_{HL}) acts as the primary trigger group. Without this ionization, the conformational change cannot occur [i.e., k_f = 0 when the pH is significantly below pK_{HL}; we note that thermodynamic data are also consistent with ionization of His73 controlling formation of the His73 alkaline conformer[6,31] (see also Figure 3B and Table 1)]. Two other ionizable groups (pK_{H1} and pK_{H2}) act to modulate the barrier height for the conformational transition. Thus, as the pH is varied, the pK_{HL} ionization allows the alkaline transition to proceed in the forward direction (k_f) and pK_{H1} and pK_{H2} change the magnitudes of k_f and k_b from k_{f1} and k_{b1} at pH values below pK_{H1} to k_{f2} and k_{b2} at pH values between pK_{H1} and pK_{H2} to k_{f3} and k_{b3} at pH values above pK_{H2}, respectively. For the His73−heme alkaline transition of K73H and K73H/K73A iso-1-Cyt*c*, pK_{H1} is near 5.5 and pK_{H2} is near 9. pK_{HL} was found to be 6−6.5, consistent with deprotonation of the incoming His73 ligand.

The very different values of pK_H obtained by fitting the k_{obs} and amplitude data for the fast phase of our pH jump stopped-flow experiments on AcH73 to the standard mechanism for the alkaline transition (Figure 4 and Table 2) could indicate that a more complex mechanism, like the one outlined in Figure 5, is operative. Even for this more complicated mechanism, when $pK_{HL} > pK_{H1}$, the rise in the amplitude in pH jump experiments as a function of pH depends primarily on pK_{HL} because ionization of the ligand is required for formation of the alkaline

conformer.[5,6] The amplitude is affected at higher pH by pK_{H2} only if the ionization of this group significantly affects the equilibrium between the native and alkaline conformers. For the K73H variant, pK_{H2} did not perturb this equilibrium.[5] Thus, if the more complicated mechanism in Figure 5 is operative for the AcH73 variant, the fit of the fast phase amplitude data (His73−heme alkaline transition) in Figure 4A to the standard kinetic model for the alkaline transition would be expected to yield a pK_H that primarily reflects pK_{HL}. The pK_H of 6.45 ± 0.05 observed for the fast phase amplitude data, which is consistent with ionization of His73, supports this possibility. The pK_H observed for the k_{obs} versus pH data for the fast phase of the pH jump data for the AcH73 variant (Table 2) is consistent with the pK_{H2} observed in our work with the K73H and K73H/K79A variants.[5,6]

Thus, it is possible that pK_{H1} and pK_{HL} are not evident in the k_{obs} versus pH data for the fast phase in pH jump studies on the AcH73 variant (Figure 4A) because of compensating effects of pK_{H1} on k_b and of pK_{HL} on k_f leading to invariant k_{obs} for the His73−heme alkaline transition between pH 5 and 8. To test this hypothesis, an alternative means of measuring the conformational change between the native conformer (heme−Met80) and the His73−heme alkaline conformer, which permits direct measurement of the microscopic rate constants, k_f and k_b, is necessary. We have demonstrated recently that conformationally gated electron transfer (ET) between iso-1-Cyt*c* and the small molecule inorganic reductant, hexaammineruthenium(II) chloride (a_6Ru^{2+}), could be used to directly measure k_f and k_b at pH 7.5 for the His73−heme alkaline transition of the AcH73 variant (see Figure 6).[15]

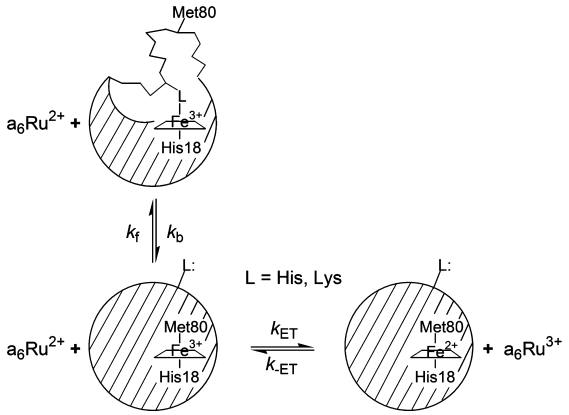

Figure 6. Schematic representation of the kinetic mechanism for conformationally gated ET between a_6Ru^{2+} and the heme of Cyt*c*. Rate constants are defined in the text.

To assess whether k_f and k_b vary as a function of pH from pH 5 to 8 where k_{obs} ($=k_f + k_b$) obtained by pH jump methods is independent of pH (Figure 4A), we have extended our conformationally gated ET measurements on the AcH73 variant to cover the range from pH 5 to 9. Over this pH range, significant amounts of both native (Met80−heme) and alkaline (His73−heme and Lys79−heme) conformers are expected to be in equilibrium (Figure 3). Thus, after the oxidized AcH73 and a_6Ru^{2+} solutions had been rapidly mixed, kinetic phases due to both bimolecular ET with the native conformer and conformationally gated ET with alkaline conformers are expected. As the pH is changed, the amplitudes of the kinetic phases due to each conformation will reflect the changing equilibrium populations of the native and alkaline conformers. Thus, kinetic amplitudes from the ET measurement provide a check of the validity of the thermodynamic model (Figure 3A) used to fit our equilibrium pH titration data (Figure 3B).

The observed rate constant for bimolecular ET with the native conformer, $k_{obs,ET}$, should be linearly dependent on a_6Ru^{2+} concentration, with the bimolecular ET rate constant, k_{ET}, as the slope (eq 5; see Figure 6)

$$k_{obs,ET} = k_{ET}[a_6Ru^{2+}] \quad (5)$$

This treatment assumes k_{-ET} is negligible, which is reasonable given the difference in the redox potential between iso-1-Cyt*c* ($E^{o\prime}$ = 290 mV vs NHE[17]) and a_6Ru^{2+} (E^{o} = 50 mV vs NHE[58]) and the large molar excess (~100−5000-fold) of a_6Ru^{2+} over iso-1-Cyt*c* in our experiments. Direct bimolecular ET with a_6Ru^{2+} is not expected for Lys−heme alkaline conformers because of the low reduction potential near −200 mV versus NHE for Lys−heme conformers.[17,59] Estimates of the reduction potential of bis-His Cyt*c* range from 0 to 50 mV versus NHE.[60−62] Thus, direct bimolecular ET might be possible, but in our previous studies of both His73−heme and His79−heme conformers of iso-1-Cyt*c*, we observe no evidence of direct bimolecular ET to His−heme alkaline conformers; the data clearly show that ET to these His−heme conformers is limited by the rate constant k_b (see Figure 6) for the conformational change back to the native Met80−heme conformer.[15,63,64] Thus, both His−heme and Lys−heme[65−67] alkaline conformers must first return to the native state before reduction of the heme can occur. It is important to remember that k_{ET} in eq 5 depends not only on the $\Delta E^{o\prime}$ for the redox reaction between the inorganic reagent and the protein but also on the equilibrium constant for and electronic coupling in the precursor complex between the inorganic redox reagent and the redox protein.[68,69] Evidently for the His−heme alkaline conformers, the nature of the precursor complex with a_6Ru^{2+} disfavors bimolecular ET.

Thus, for both Lys−heme and His−heme alkaline conformers, ET is conformationally gated, requiring formation of the native state (Met80−heme). In both cases, reduction of the heme is expected to produce a hyperbolic dependence of the observed rate constant, $k_{obs,gated}$, on a_6Ru^{2+} concentration as given by eq 6, which is derived using the steady-state

$$k_{obs} = \frac{k_{ET}k_b[a_6Ru^{2+}]}{k_{ET}[a_6Ru^{2+}] + k_f} \quad (6)$$

approximation[70−72] where k_b is the rate constant for formation of the native (Met80−heme) conformer from either the His73−heme or Lys79−heme alkaline conformer and k_f is the rate constant for formation of alkaline conformers (His73−heme or Lys79−heme) from the native conformer. In eq 6, k_{ET} corresponds to the direct bimolecular ET to the native (heme−Met80) state of the protein. k_f and k_b in Figure 6 are defined to be mechanistically equivalent to k_f and k_b, respectively, in eq 2 (and Figure 5) for analysis of the pH jump kinetics of the alkaline transition; thus, the pH dependence of both k_f and k_b will depend on the details of the mechanism of the conformational change between the native state and the His73−heme alkaline conformer. At high a_6Ru^{2+} concentrations, $k_{obs,gated}$ in eq 6 asymptotically approaches k_b (conformationally gated ET), and at low a_6Ru^{2+} concentrations, $k_{obs,gated}$ becomes linearly dependent on a_6Ru^{2+} concentration with a

slope of $k_{ET}(k_b/k_f)$ (coupled ET[73,74]). Thus, if k_{ET} is known from fits of direct bimolecular ET data for the native conformer to eq 5, both k_f and k_b can be obtained from fits of eq 6 to the a_6Ru^{2+} concentration dependence of $k_{obs,gated}$ for reduction of AcH73 iso-1-Cytc. The steady-state approximation used in deriving eq 6 requires $k_{ET}[a_6Ru^{2+}] + k_f \gg k_b$.[75] An improved steady-state approximation,[75] which changes the denominator in eq 6 to $k_{ET}[a_6Ru^{2+}] + k_f + k_b$, can also be used. However, at low a_6Ru^{2+} concentrations where $k_{ET}[a_6Ru^{2+}] + k_f \gg k_b$ no longer holds and $k_{ET}[a_6Ru^{2+}]$, k_f, and k_b are similar in magnitude, both the steady-state approximation and the improved steady-state approximation deviate from the exact solution to the kinetic mechanism in Figure 6.[75] Thus, at low a_6Ru^{2+} concentrations, we have used numerical methods to directly fit kinetic traces to the mechanism in Figure 6. In Discussion, we show that numerical methods and the steady-state approximation (eq 6) yield qualitatively similar values for k_f.

Rate Constant Data from Conformationally Gated Electron Transfer Measurements of the AcH73 Variant. Reduction of the oxidized AcH73 variant by a_6Ru^{2+} was followed via the increase in the absorbance of the redox-sensitive 550 nm band of Cytc as shown for data at pH 5.5 in Figure 7. Four kinetic phases are clearly evident (see data at

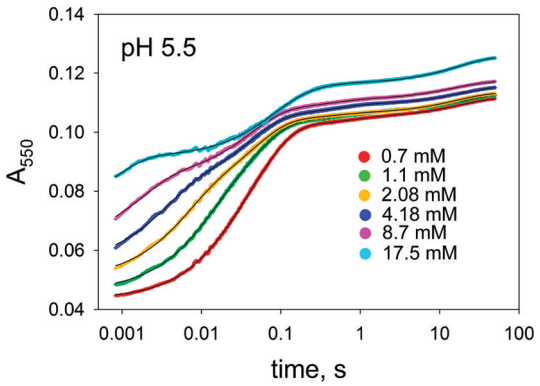

Figure 7. Plots of absorbance at 550 nm, A_{550}, vs time (on a logarithmic scale) for reduction of the AcH73 variant of iso-1-Cytc by a_6Ru^{2+} at 25 °C and pH 5.5 (10 mM acetic acid and 0.1 M NaCl). Kinetic data at six different concentrations of a_6Ru^{2+} are shown. The solid lines are fits to a quadruple-exponential rise to maximum equation. Rate constant and amplitude parameters from these fits are listed in Tables S8–S11 of the Supporting Information. Data at other pH values are presented in Figure S8 of the Supporting Information. An increase in the background absorbance due to a_6Ru^{2+} is apparent as the concentration of a_6Ru^{2+} increases.

4.18 and 8.7 mM a_6Ru^{2+}, in particular). In general, at all pH values, better fits are obtained with a four-exponential equation than with a three-exponential equation (Figure S7 of the Supporting Information). The observed rate constant for the fastest phase, $k_{obs,1}$, is linearly dependent on a_6Ru^{2+} concentration (see Figure S9 of the Supporting Information) at all pH values, as expected for bimolecular ET (eq 5) with the native state of the AcH73 variant. From pH 5 to 7, k_{ET} is in the range of 60–70 mM^{-1} s^{-1}. From pH 7.5 to 9, k_{ET} decreases to the range of 45–55 mM^{-1} s^{-1} (Figure S10 of the Supporting Information). This decrease could be related to deprotonation of His73, because bimolecular ET with inorganic redox reagents is sensitive to protein surface charge.[76] However, we cannot rule out the possibility that the decrease in k_{ET} at higher pH is an artifact of the reduced amplitude of this phase due to the smaller population of the native conformer at higher pH (see Figure S8 of the Supporting Information). The k_{ET} for the native conformer of the AcH73 variant is comparable to the k_{ET} observed previously for horse heart Cytc[77] and for WT and the K73H variant of iso-1-Cytc.[64]

The faster of the two intermediate phases for the reduction of the AcH73 variant by a_6Ru^{2+}, $k_{obs,2}$, shows saturation behavior as a function of a_6Ru^{2+} concentration across the range of pH 5–9 studied here (Figure 8), as would be expected for

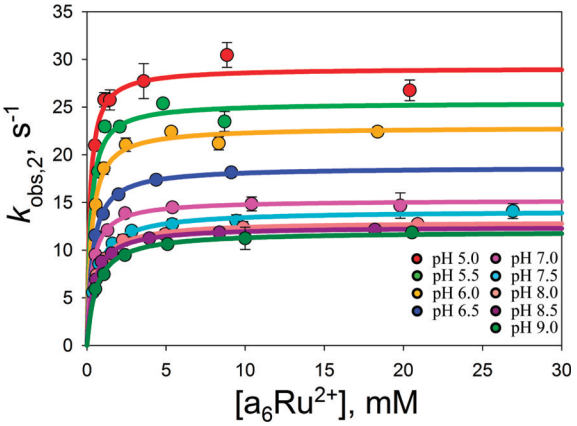

Figure 8. Plots of $k_{obs,2}$ vs a_6Ru^{2+} concentration for the reaction of a_6Ru^{2+} with the oxidized AcH73 variant from pH 5 to 9 in 10 mM buffers containing 0.1 M NaCl at 25 °C. The solid lines are fits to eq 6, which gives values for k_b and k_f as defined in Figure 6. k_b and k_f from these fits are listed in Table S12 of the Supporting Information.

conformational gating of ET when the protein is in the His73–heme alkaline state. Fits of these data to eq 6 using k_{ET} obtained from $k_{obs,1}$ data are shown in Figure 8. It is evident in Figure 8 that as the pH decreases toward 5, $k_{obs,2}$ levels out at progressively larger magnitudes. Because eq 6 reduces to k_b at high a_6Ru^{2+} concentrations, the plots in Figure 8 indicate that k_b for the conformational change from the His73–heme alkaline state to the ET active Met80–heme native state (see Figure 6) increases at lower pH.

The second intermediate phase, $k_{obs,3}$, is a low-amplitude phase that shows saturation behavior as a function of a_6Ru^{2+} concentration at pH <7.5 (Figure S11 and Table S10 of the Supporting Information). At pH >7.5, $k_{obs,3}$ appears to be independent of a_6Ru^{2+} concentration [$k_f = 0$ within error when the data are fit to eq 6 (see Table S13 of the Supporting Information)]. The limiting magnitude of $k_{obs,3}$ at high concentrations of a_6Ru^{2+} decreases significantly at pH >7.5 (Figure S11 and Table S13 of the Supporting Information). This pH-dependent change in behavior suggests that the species corresponding to $k_{obs,3}$ may differ at acidic versus alkaline pH. The change in the magnitude of $k_{obs,3}$ is small relative to the error in the data; thus, in general, k_f derived from fits of the data to eq 6 is poorly determined (Table S13 of the Supporting Information). However, at pH <7.5, the magnitude of k_f for the species corresponding to $k_{obs,3}$ is roughly similar in magnitude to k_f derived from $k_{obs,2}$ for formation of the His73–heme alkaline conformer. In contrast to k_f for the His73–heme alkaline conformer, k_f for the species corresponding to $k_{obs,3}$ appears to increase as the pH decreases. Thus, at lower pH values, this species may correspond to the acid-unfolded state or an intermediate along the path to the acid-unfolded state.

dx.doi.org/10.1021/bi201082h | Biochemistry 2011, 50, 10027–10040

The nature of the species corresponding to $k_{obs,3}$ at alkaline pH is unclear.

The slowest kinetic phase for reduction of the AcH73 variant by a_6Ru^{2+} likely arises from different species in acidic versus basic solutions, too. When $k_{obs,4}$ versus a_6Ru^{2+} concentration is fit to the conformationally gated ET scheme in Figure 6, the magnitude of k_f is zero or near zero within error from pH 5.5 to 7.5 (Figure S12 and Table S14 of the Supporting Information). In essence, we are unable to detect any dependence of $k_{obs,4}$ on a_6Ru^{2+} concentration in this pH range. A possible explanation for this behavior is that $k_{obs,4}$ is due primarily to a His73–heme alkaline conformer with a *cis*-peptidyl–prolyl bond up to pH 7.5, such that $k_{obs,4}$ is limited by isomerization of a *cis*-peptidyl–prolyl bond back to the *trans*-peptidyl–prolyl bond, which would be required for formation of the native (Met80–heme) state of the AcH73 variant from a His73–heme alkaline conformer with a *cis*-peptidyl–prolyl bond.[5,6] Repopulation of a His73–heme alkaline conformer with a *cis*-peptidyl–prolyl bond would require very slow *trans* to *cis* peptidyl–prolyl bond isomerization (very small k_f in eq 6); thus, $k_{obs,4} \approx k_b$ over the a_6Ru^{2+} concentration range used for our measurements. From pH 5 to 7.5, k_b is ~0.06 s^{-1}, similar to the rate constant of 0.052 ± 0.001 s^{-1} that we have observed for isomerization of a *cis*-peptidyl–prolyl bond back to the *trans* conformer in pH jump studies of the return of the His73–heme alkaline conformer to the native state for the K73H/K79A variant of iso-1-Cytc.[6] For pH 8–9, $k_{obs,4}$ as a function of a_6Ru^{2+} concentration shows saturation behavior. Fits of the data to eq 6 yield non-zero values of k_f that increase with pH (Figure S12 and Table S14 of the Supporting Information). This behavior is consistent with $k_{obs,4}$ being due primarily to the Lys79–heme alkaline conformer in this pH range.

Amplitude Data from Conformationally Gated Electron Transfer Measurements of AcH73 Iso-1-Cytc. As noted above, the amplitudes of the phases in our ET data should reflect the equilibrium populations of the various conformers of the AcH73 variant at the pH of the ET experiment. Thus, in combination with the equilibrium data in Figure 3, the amplitude data for each phase can be used to confirm our assignment of the four ET phases we observe for the reduction of AcH73 by a_6Ru^{2+}. Fractional amplitudes (f_{amp}) as a function of pH are plotted for all four phases at ~5 mM a_6Ru^{2+} in Figure 9. We use 5 mM a_6Ru^{2+} amplitude data because the steady-state approximation in eq 6 holds under these conditions, and therefore, amplitudes directly report on relative concentrations of species in solution. The fractional amplitudes corresponding to $k_{obs,1}$, $k_{obs,2}$, and $k_{obs,4}$ ($f_{amp,1}$, $f_{amp,2}$, and $f_{amp,4}$, respectively) vary strongly with pH, whereas the variation in the fractional amplitude of $k_{obs,3}$ ($f_{amp,3}$) is relatively modest. For comparison, we have plotted the fractional populations, f_{pop}, of the native conformer (Met80–heme, dashed red line), His73–heme alkaline conformer (dashed green line), and Lys79–heme alkaline conformer (dashed pink line) derived from the thermodynamic parameters listed in Table 1 (0 M gdnHCl) obtained by fitting the data in Figure 3B to the thermodynamic model in Figure 3A.

The pH-dependent behavior of $f_{amp,1}$ corresponds qualitatively to the pH-dependent f_{pop} of the native state predicted by the thermodynamic parameters listed in Table 1 (solid red line and data points vs red dashed line). The pH dependence of f_{pop} for the native state of AcH73 predicted by our thermodynamic parameters is uniformly higher than the $f_{amp,1}$ by an approximately constant amount throughout the pH range

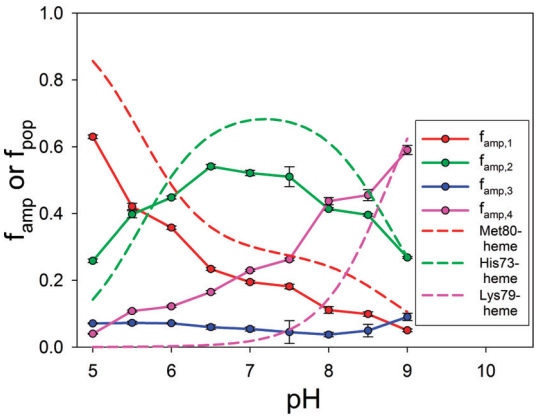

Figure 9. Plots of fractional amplitude (f_{amp}) as a function of pH for the phases obtained from a fit to a four-exponential rise to maximum equation at ~5 mM a_6Ru^{2+} (data points with error bars connected by solid lines). With ~5 mM a_6Ru^{2+} data, all four phases are well separated and the fast phase amplitude could still be evaluated reliably (Figure 7 and Figure S8 of the Supporting Information). The dashed lines show the fractional populations, f_{pop}, of the native (Met80–heme) and alkaline (His73–heme and Lys79–heme) forms predicted using the thermodynamic parameters in Table 1 (0 M gdnHCl) derived from a fit of the thermodynamic model in Figure 3A to the data in Figure 3B.

from 5 to 9. This discrepancy is in part attributable to the fact that the thermodynamic model in Figure 3A does not contain a species corresponding to $f_{amp,3}$ in our ET data. It is also possible that our estimate of the difference between ε_N and ε_{alk} (0.53 mM^{-1} cm^{-1}) for the AcH73 variant based on previous work with the K73H variant is slightly inaccurate. However, the good qualitative correspondence between the pH dependencies of $f_{amp,1}$ and f_{pop} for the native state of AcH73 confirms our assignment of $k_{obs,1}$ to direct bimolecular ET to AcH73 molecules that are in the native state at the time of mixing with the a_6Ru^{2+} reductant.

The pH dependence of $f_{amp,2}$ (green line and data points, Figure 9) agrees qualitatively with the pH dependence of f_{pop} for the His73–heme alkaline conformer (green dashed line) based on the thermodynamic parameters listed in Table 1. In the pH range of 6–8, $f_{amp,2}$ is uniformly low relative to f_{pop} for the His73–heme alkaline conformer. We note that our previous studies have shown that an X–Pro peptidyl–prolyl bond partially isomerizes from *trans* to *cis* when the His73–heme alkaline conformer forms.[5,6] The magnitude of f_{pop} for the His73–heme alkaline conformer measured under equilibrium conditions will reflect His73–heme alkaline conformers with both the *cis* and *trans* X–Pro peptidyl–prolyl bonds. In conformationally gated ET measurements, the His73–heme alkaline conformer is expected to divide into fast (*trans*-X–Pro) and slow (*cis*-X–Pro) phases. The reduced magnitude of $f_{amp,2}$ relative to f_{pop} for the His73–heme alkaline conformer is thus attributable to peptidyl–prolyl bond isomerization. Given that $k_{obs,2}$ is the second fastest ET phase, we assign this phase to a His73–heme alkaline conformer with a *trans*-X–Pro bond that must return to the native (Met80–heme) conformer before it can be reduced by a_6Ru^{2+}.

The magnitude of $f_{amp,3}$ is small at all pH values studied (blue line in Figure 9). As discussed in the previous section, the source of this kinetic phase is unclear and the species involved may vary with pH. In line with this possibility, $f_{amp,3}$ decreases slightly from pH 5 to 8 and then increases from pH 8 to 9.

The pH dependence of the fractional amplitude of the slowest phase, $f_{amp,4}$ (pink line and data points, Figure 9), qualitatively behaves like the pH dependence of f_{pop} for the Lys79−heme alkaline conformer. However, below pH 6.5, f_{pop} for the Lys79−heme alkaline conformer is predicted to be essentially zero based on the thermodynamic parameters listed in Table 1, in contrast to the significant magnitude actually observed for $f_{amp,4}$. We note that from pH 5 to 6.5, $f_{amp,4}$ grows in synch with $f_{amp,2}$, consistent with the slow phase being due to a His73−heme alkaline conformer with a *cis*-X−Pro peptide bond. From pH 5.5 to 6.5, the ratio $f_{amp,4}/(f_{amp,2} + f_{amp,4})$ is 0.21−0.23, consistent with the ∼20% population of *cis*-proline conformers in the His73−heme alkaline state observed in our previous studies of K73H/K79A iso-1-Cyt*c*.[6] Thus, at lower pH values, this slow phase is attributable to a His73−heme alkaline conformer with a *cis*-X−Pro bond. Thus, the *cis* to *trans* peptidyl−prolyl bond isomerization is rate-limiting for the return to the a_6Ru^{2+}-reducible native state of the AcH73 variant. At higher pH values, $f_{amp,4}$ becomes the dominant phase consistent with assignment of this phase to the Lys79−heme alkaline conformer. As with the His73−heme conformer, the behavior of $k_{obs,4}$ as a function of a_6Ru^{2+} concentration above pH 7.5 is consistent with the requirement that the Lys79−heme alkaline conformer isomerize to the native (heme−Met80) species before it can be reduced by a_6Ru^{2+}.

DISCUSSION

Comparison of the Kinetic Mechanism of Formation of the His73−Heme Conformer from the Native State of Iso-1-Cyt*c* with and without His26. Figure 10 compares the pH dependence of k_f and k_b measured by conformationally gated ET methods for the transition between the native state and the His73−heme alkaline state (*trans*-X−Pro) of the AcH73 variant to pH jump measurements of the same conformational transition for both the AcH73 and K73H variants. We show k_f values obtained using the steady-state approximation ($k_{f,ss}$, from fits of eq 6 to the data in Figure 8) and obtained by numerical fitting ($k_{f,num}$) of kinetic data at ∼1 mM a_6Ru^{2+} (Tables S15 and S16 and Figures S13 and S14 of the Supporting Information). At low pH values, where the concentration of the oxidized Met80−heme conformer is highest, the deviation between $k_{f,ss}$ and $k_{f,num}$ is largest. However, for the most part, the numerical fitting results indicate that the effect of the breakdown of the steady-state approximation on the values of k_f extracted from fitting the data in Figure 8 to eq 6 is small. We note that the sum of k_f and k_b (=k_{obs}, blue triangles using $k_{f,ss}$ and green inverted triangles using $k_{f,num}$ in Figure 10) obtained by ET methods is within error identical to k_{obs} measured by pH jump methods for the transition between the native state and the His73−heme alkaline state for AcH73 iso-1-Cyt*c*. The significance of the close agreement between the sum of k_f and k_b derived from ET measurements and k_{obs} from pH jump experiments is 2-fold. First, it confirms the validity of the conformationally gated ET mechanism in Figure 6 used to analyze the data in Figure 8. The close agreement between k_{obs} (=k_f + k_b) from pH jump experiments (directly monitors the kinetics of the conformational change between the native state and the His73−heme alkaline state) and the sum of k_f and k_b (=k_{obs}) obtained from analysis of the data in Figure 8 with the kinetic model in Figure 6 indicates that the pH jump and ET experiments are probing the same conformational change, the His73−heme alkaline transition. Second, it is clear that the apparent consistency of the k_{obs} versus pH data from pH jump experiments with the standard model for the alkaline conformational transition (eq 2)[4] is due to coincidental compensation between decreasing k_b and increasing k_f as pH increases. The observation that both k_f and k_b for the interconversion between the native state and the His73−heme alkaline conformer vary significantly at pH <8 demonstrates definitively that the standard kinetic model for the alkaline conformational transition is insufficient in this case. Our analysis in Results of the discrepancy between the pK_H derived from the amplitude and the k_{obs} data provided estimates of pK_{HL} and pK_{H2}, respectively, based on the assumption that the mechanism in Figure 5 involving three ionizable groups was actually operative for the His73−heme alkaline transition of the AcH73 variant. Our conformationally gated ET data demonstrate the validity of our hypothesis that the effects of pK_{HL} on k_f and pK_{H1} on k_b compensate to produce an invariant k_{obs} between pH 5 and 8 in our pH jump measurements.

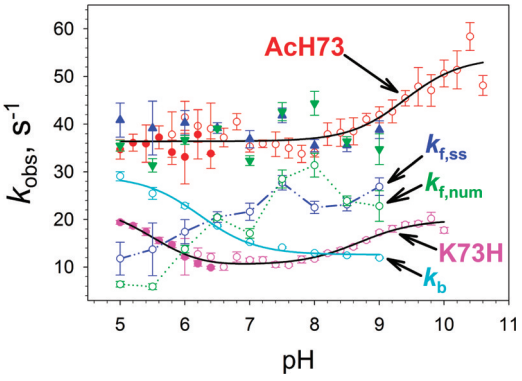

Figure 10. Plots of k_b (cyan), $k_{f,ss}$ (blue, steady-state approximation), and $k_{f,num}$ (green, numerical fitting) vs pH obtained from conformationally gated ET measurements for the conformational transition between the native state and the His73−heme alkaline state (*trans*-X−Pro bond) for AcH73 iso-1-Cyt*c*. The sum of $k_{f,ss}$ and k_b (=k_{obs}) from conformationally gated ET measurements is shown with solid blue triangles. The sum of $k_{f,num}$ and k_b (=k_{obs}) from conformationally gated ET measurements is shown with solid inverted green triangles. Plots of k_{obs} vs pH from pH jump measurements of the conformational transition from the native state to the His73−heme alkaline state for the AcH73 (red) and K73H[5] (pink) variants of iso-1-Cyt*c* are shown for comparison. The solid black curve through the pH jump data for the AcH73 variant is a fit of the data to eq 2 in Experimental Procedures. The solid black curve through the pH jump data from the K73H variant is a fit of the data to the kinetic model in Figure 5. The solid cyan curve through the k_b vs pH data is a fit of the data to eq 7.

Because k_b is affected only by pK_{H1} from pH 5 to 9, the k_b data in Figure 10 can be used to estimate the pK_{H1} for the His73−heme alkaline transition of the AcH73 variant. The effect of pK_{H1} on the pH dependence of k_b is given by eq 7 (parameters defined in Figure 5).[5,43] A fit of eq 7 to the pH dependence of k_b (solid cyan line, Figure 10) yields the following: k_{b1} = 29.1 ± 0.7 s^{-1}, k_{b2} = 12.6 ± 0.4 s^{-1}, and pK_{H1} = 6.2 ± 0.1.

$$k_b = \frac{k_{b1}[H^+] + k_{b2}K_{H1}}{K_{H1} + [H^+]} \quad (7)$$

The magnitude of pK_{H1} is within the range of 5−6.4 observed for the K73H and K73H/K79A variants of iso-1-Cyt*c*. Combining our results from conformationally gated ET and

pH jump measurements, we find the kinetics of the His73−heme alkaline transition are consistent with the kinetic model in Figure 5 ($pK_{H1} \sim 6.2$, $pK_{HL} \sim 6.5$, and $pK_{H2} \sim 9.4$). Thus, for the AcH73, K73H, and K73H/K79A variants of iso-1-Cyt*c*, three ionizable groups affect the kinetics of the His73−heme alkaline transition.

We also note that the ratio k_f/k_b [$=K_{C1}/(1 + K_{iso})$, where K_{iso} is the equilibrium constant for *trans*- to *cis*-peptidyl−prolyl bond isomerization] obtained by conformationally gated ET measurements on the His73−heme alkaline conformer is ∼2 at and above pH 7.5 (Table S12 of the Supporting Information) where this conformer will be fully populated. If we use a pK_{C1} of −0.41 (Table 1) from our thermodynamic analysis of the His73−heme alkaline transition and assume the *cis*-X−Pro bond is ∼20% populated in the His73−alkaline conformer[6] ($K_{iso} \sim 0.25$), we obtain $K_{C1}/(1 + K_{iso}) \sim 2.1$. This comparison demonstrates that our conformationally gated ET measurements are also consistent with our independent thermodynamic measurements of the native to His73−heme alkaline transition of the AcH73 variant.

The observation that variants of iso-1-Cyt*c* with (K73H and K73H/K79A) and without (AcH73) His26 have kinetics for the His73−heme alkaline transition affected by the pK_{H1} ionization shows that His26 (pK_a shifted to ∼3.5 in native Cyt*c*[37,38]) is not responsible for the pK_{H1} ionization in the mechanism (Figure 5) of the His73−heme alkaline transition. The heme propionates are known to have shifted pK_a values in mitochondrial Cyt*c* and thus are also possible candidates for the ionizable group responsible for pK_{H1}. The inner propionate (HP-7) is believed to have a pK_a of <4.5, and it has been suggested that the outer propionate [heme propionate 6 (HP-6)] has a pK_a of >9.[1,39,40] The intrinsic pK_a values of the heme propionates are predicted to be 4.8 and 5.6.[38] Thus, pK_{H1} could readily result from the titration of a heme propionate in either the alkaline form or the transition state between the native and alkaline forms of the protein.

Protonation of both His26 and HP-7 destabilizes the Infrared foldon at low pH, whereas the effect of low pH on the Red foldon is less pronounced.[26] However, formation of the alkaline state appears to require opening of the Infrared foldon,[30] whereas in the final alkaline state, the primary disruption is to the Red foldon.[20] Protonation of HP-7 in an intermediate with the Infrared foldon transiently opened might be expected to be more facile than in either end state of the alkaline conformational transition, leading to a lowering of the transition-state barrier relative to the end states as the pH decreases near the intrinsic pK_a of HP-7.

Effect of Global Destabilization on the Kinetics of the Alkaline Transition. In our previous report, we observed that near neutral pH, global destabilization of iso-1-Cyt*c* lowered the barrier for the native to His73−heme alkaline transition.[15] The results presented here show that lower global stability lowers this barrier across a broad pH range as shown by the comparison of k_{obs} for the native to His73−heme alkaline transition of the less stable AcH73 variant versus the more stable K73H variant of iso-1-Cyt*c* (Figure 10). This observation is consistent with the general observation that the dynamics of the less stable proteins from cold-adapted (psychrophilic) organisms are faster than for the more stable proteins of mesophilic organisms when measured at the same temperature.[78] Thus, His26 may act as a stabilizing brace between the least stable Infrared foldon and the Green foldon (Figure 1) that also serves to slow the dynamics of conformational transitions in Cyt*c*. However, it is possible that the primary effect on the barrier to the alkaline transition is the destabilization of the Infrared foldon,[29] which is implicated in promoting the alkaline transition,[30] and that the loss of global stability is simply a result of the sequential unfolding of the foldons[25−27] and not the cause of enhanced dynamics for AcH73 iso-1-Cyt*c*. Study of variants that affect global stability without affecting the stability of the Infrared substructure will be important in sorting out the relative role of local versus global effects on protein dynamics.

Species Present during the Alkaline Transition. The alkaline transition of Cyt*c* has normally been interpreted in terms of a model involving a native state with heme−Met80 ligation and an alkaline state with one primary lysine ligand bound or multiple lysine ligands competing for the sixth coordination site of the heme.[17−19,79] While the existence of a transient intermediate with neither Met80 nor a lysine bound to the heme is likely,[80] electrochemical,[13,14] vibrational,[7,10−12] and magnetic circular dichroism[8,9] studies have shown evidence for a significant equilibrium population of species other than the native state or lysine−heme alkaline conformers. It is likely that Met80 remains bound to heme in these intermediates (termed 3.5[7] or III*[8]), although in a non-native conformation.[7,8]

Our conformationally gated ET data allow us to probe the equilibrium population of species based on their differential reactivities with the a_6Ru^{2+} redox reagent. The decrease in the population of the species with native-state redox properties (Figure 9, red line) is consistent with the decrease in 695 nm absorbance in Figure 3 (also red dashed line in Figure 9). The thermodynamic parameters in Table 1 (0 M gdnHCl, green dashed line in Figure 9) predict that the His73 form will grow and reach a maximum fractional population of ∼0.65 in the pH range of 6.5−7.5 ($f_{amp,2} + f_{amp,4} \approx 0.7$ at pH 6.5, where $f_{amp,4}$ is still predominately due to the His73−heme conformer with a *cis*-X−Pro bond). Above pH 7.5, the thermodynamic parameters listed in Table 1 predict that the His73−heme conformer decreases in population (green dashed line, Figure 9) in favor of the Lys79−heme conformer with the Lys79−heme conformer (pink dashed line, Figure 9) becoming dominant above pH 8.6. Thus, our thermodynamic model for fitting the data in Figure 3 is consistent with the speciation as a function of pH as observed with the f_{amp} data in Figure 9. Given that the III* intermediate form likely has the lower redox potential associated with the alkaline state,[8,14] our gated ET data are consistent with direct conversion of the Met80−heme form to the His73−heme alkaline conformer without significant population of an intermediate like III*. We note that this work was conducted with yeast iso-1-Cyt*c* rather than with horse Cyt*c* used in the studies that revealed the 3.5 or III* intermediate and that the His73−heme alkaline conformer is populated at lower pH than the 3.5 or III* intermediate. However, the pK_{H2} of 9.4 observed for the AcH73 variant and the pK_{H2} range of 8.7−9.2 observed in our previous work with K73H, K73H/K79A, and K79H iso-1-Cyt*c* variants[3,5,6,43] are similar to the p*K* values of 8.5−8.7 observed for formation of the III* and 3.5 intermediates. Thus, an intermediate like III* or 3.5 may promote formation of the His73−heme alkaline conformer at higher pH.

Our conformationally gated ET data do show evidence for a fourth low-amplitude species, which as noted above may result from different species in the acid versus the alkaline region of our measurements. For the K73H/K79A variant, equilibrium

pH titration data show that a high-spin species grows in at pH >8.5 (shoulder near 605 nm).[6] Thus, in the absence of Lys, other species clearly can compete with His73 for heme binding, displacing it at higher pH values. From this work and previous work, it is evident that the pH-dependent conformational behavior of Cyt*c* in the pH regime associated with the alkaline transition is complex and affected by multiple ionizable groups.

CONCLUSIONS

We have shown that conformationally gated ET methods provide a powerful approach for probing the dynamics of conformational changes in redox active proteins. In this work, the method has allowed us to demonstrate that His26 is not the source of the low-pH ionization that modulates the dynamics of the native to His73−heme alkaline transition of iso-1-Cyt*c*. A likely alternate candidate is HP-7. The results further confirm that three ionizations impact heme ligand-exchange reactions of mitochondrial Cyt*c* in the pH range of 5−10. Our data also show that decreasing the global stability of iso-1-Cyt*c* enhances conformational dynamics in analogy to the behavior of cold-adapted enzymes from psychrophilic organisms. Further studies are underway to probe whether global stability is a universal modulator of local conformational dynamics.

ASSOCIATED CONTENT

Supporting Information

Representative equilibrium data, pH jump kinetic data, and conformationally gated electron transfer kinetic data for the alkaline transition of the AcH73 variant; tables of equilibrium and kinetic parameters for the alkaline transition of the AcH73 variant; and detailed experimental procedures for numerical fitting of conformationally gated electron transfer data. This material is available free of charge via the Internet at http://pubs.acs.org.

AUTHOR INFORMATION

Corresponding Author

*Telephone: (406) 243-6114. Fax: (406) 243-4227. E-mail: bruce.bowler@umontana.edu.

Present Address

[†]Department of Pharmaceutical Sciences, University of Colorado School of Pharmacy, Aurora, CO 80045.

Funding

This research was supported by National Science Foundation Grants CHE-0316378 and CHE-0616656.

ACKNOWLEDGMENTS

We thank Dr. Melisa Cherney for valuable discussions.

ABBREVIATIONS

Cyt*c*, cytochrome *c*; a_6Ru^{2+}, hexaammineruthenium(II) chloride; gdnHCl, guanidine hydrochloride; $\Delta G^{\circ}_{u}(H_2O)$, free energy of unfolding in the absence of denaturant; *m* value, slope of a plot of the free energy of unfolding versus denaturant concentration; HP-7, heme propionate 7, also known as the inner heme propionate and heme propionate A; HP-6, heme propionate 6, also known as the outer heme propionate and heme propionate D; HX, hydrogen exchange; WT, wild-type protein carrying the Cys102 → Ser mutation. Protein variants are abbreviated by the one-letter code for the wild-type amino acid followed by the position number and then the one-letter code for the amino acid replacing the wild-type amino acid. For example, the variant in which lysine 73 is replaced with histidine is designated K73H. AcH73 is an iso-1-cytochrome *c* variant in which Ac indicates that it contains mutations that lead to N-terminal acetylation in vivo, and H73 indicates a K73H mutation. Other mutations in this variant are described in the text.

REFERENCES

(1) Moore, G. R., and Pettigrew, G. W. (1990) *Cytochromes c: Evolutionary, Structural and Physicochemical Aspects*, Springer-Verlag, New York.

(2) Wilson, M. T., and Greenwood, C. (1996) The alkaline transition in ferricytochrome *c*. In *Cytochrome c: A Multidisciplinary Approach* (Scott, R. A., and Mauk, A. G., Eds.) pp 611−634, University Science Books, Sausalito, CA.

(3) Cherney, M. M., and Bowler, B. E. (2011) Protein dynamics and function: Making new strides with an old warhorse, the alkaline conformational transition of cytochrome *c*. *Coord. Chem. Rev. 255*, 664−677.

(4) Davis, L. A., Schejter, A., and Hess, G. P. (1974) Alkaline isomerization of oxidized cytochrome *c*. Equilibrium and kinetic measurements. *J. Biol. Chem. 249*, 2624−2632.

(5) Martinez, R. E., and Bowler, B. E. (2004) Proton-mediated dynamics of the alkaline conformational transition of yeast iso-1-cytochrome *c*. *J. Am. Chem. Soc. 126*, 6751−6758.

(6) Baddam, S., and Bowler, B. E. (2005) Thermodynamics and kinetics of formation of the alkaline state of a Lys 79 → Ala/Lys 73 → His variant of iso-1-cytochrome *c*. *Biochemistry 44*, 14956−14968.

(7) Weinkam, P., Zimmermann, J., Sagle, L. B., Matsuda, S., Dawson, P. E., Wolynes, P. G., and Romesberg, F. E. (2008) Characterization of alkaline transitions in ferricytochrome *c* using carbon-deuterium infrared probes. *Biochemistry 47*, 13470−13480.

(8) Verbaro, D., Hagarman, A., Soffer, J., and Schweitzer-Stenner, R. (2009) The pH dependence of the 695 nm charge transfer band reveals the population of an intermediate state of the alkaline transition of ferricytochrome *c* at low ion concentrations. *Biochemistry 48*, 2990−2996.

(9) Hagarman, A., Duitch, L., and Schweitzer-Stenner, R. (2008) The conformational manifold of ferricytochrome *c* explored by visible and far-UV electronic circular dichroism spectroscopy. *Biochemistry 47*, 9667−9677.

(10) Weinkam, P., Zimmermann, J., Romesberg, F. E., and Wolynes, P. G. (2010) The folding energy landscape and free energy excitations of cytochrome *c*. *Acc. Chem. Res. 43*, 652−660.

(11) Filosa, A., and English, A. M. (2000) Probing local thermal stabilities of bovine, horse, and tuna ferricytochromes *c* at pH 7. *J. Biol. Inorg. Chem. 5*, 448−454.

(12) Filosa, A., Ismail, A. A., and English, A. M. (1999) FTIR-monitored thermal titration reveals different mechanisms for the alkaline isomerization of tuna compared to horse and bovine cytochromes *c*. *J. Biol. Inorg. Chem. 4*, 717−726.

(13) Battistuzzi, G., Borsari, M., Ranieri, A., and Sola, M. (2002) Conservation of the free energy change of the alkaline isomerization in mitochondrial and bacterial cytochromes *c*. *Arch. Biochem. Biophys. 404*, 227−233.

(14) Battistuzzi, G., Borsari, M., Loschi, L., Martinelli, A., and Sola, M. (1999) Thermodynamics of the alkaline transition of cytochrome *c*. *Biochemistry 38*, 7900−7907.

(15) Bandi, S., and Bowler, B. E. (2008) Probing the bottom of a folding funnel using conformationally gated electron transfer reactions. *J. Am. Chem. Soc. 130*, 7540−7541.

(16) Ferrer, J. C., Guillemette, J. G., Bogumil, R., Inglis, S. C., Smith, M., and Mauk, A. G. (1993) Identification of Lys79 as an iron ligand in one form of alkaline yeast iso-1-ferricytochrome *c*. *J. Am. Chem. Soc. 115*, 7507−7508.

(17) Rosell, F. I., Ferrer, J. C., and Mauk, A. G. (1998) Proton-linked protein conformational switching: Definition of the alkaline conforma-

tional transition of yeast iso-1-ferricytochrome *c*. *J. Am. Chem. Soc. 120*, 11234−11245.
(18) Pollock, W. B., Rosell, F. I., Twitchett, M. B., Dumont, M. E., and Mauk, A. G. (1998) Bacterial expression of a mitochondrial cytochrome *c*. Trimethylation of Lys72 in yeast iso-1-cytochrome *c* and the alkaline conformational transition. *Biochemistry 37*, 6124−6131.
(19) Maity, H., Rumbley, J. N., and Englander, S. W. (2006) Functional role of a protein foldon: An Ω-loop foldon controls the alkaline transition in ferricytochrome *c*. *Proteins 63*, 349−355.
(20) Assfalg, M., Bertini, I., Dolfi, A., Turano, P., Mauk, A. G., Rosell, F. I., and Gray, H. B. (2003) Structural model for an alkaline form of ferricytochrome *c*. *J. Am. Chem. Soc. 125*, 2913−2922.
(21) Döpner, S., Hildebrandt, P., Rosell, F. I., Mauk, A. G., von Walter, M., Buse, G., and Soulimane, T. (1999) The structural and functional role of lysine residues in the binding domain of cytochrome *c* in the electron transfer to cytochrome *c* oxidase. *Eur. J. Biochem. 261*, 379−391.
(22) Döpner, S., Hildebrandt, P., Rosell, F. I., and Mauk, A. G. (1998) Alkaline conformational transitions of ferricytochrome *c* studied by resonance Raman spectroscopy. *J. Am. Chem. Soc. 120*, 11246−11255.
(23) Ow, Y. P., Green, D. R., Hao, Z., and Mak, T. W. (2008) Cytochrome *c*: Functions beyond respiration. *Nat. Rev. Mol. Cell Biol. 9*, 532−542.
(24) Jemmerson, R., Liu, J., Hausauer, D., Lam, K. P., Mondino, A., and Nelson, R. D. (1999) A conformational change in cytochrome *c* of apoptotic and necrotic cells is detected by monoclonal antibody binding and mimicked by association of the native antigen with synthetic phospholipid vesicles. *Biochemistry 38*, 3599−3609.
(25) Bai, Y., Sosnick, T. R., Mayne, L., and Englander, S. W. (1995) Protein folding intermediates: Native-state hydrogen exchange. *Science 269*, 192−197.
(26) Krishna, M. M., Lin, Y., Rumbley, J. N., and Englander, S. W. (2003) Cooperative Ω loops in cytochrome *c*: Role in folding and function. *J. Mol. Biol. 331*, 29−36.
(27) Krishna, M. M., and Englander, S. W. (2007) A unified mechanism for protein folding: Predetermined pathways with optional errors. *Protein Sci. 16*, 449−464.
(28) Michel, L. V., and Bren, K. L. (2008) Submolecular unfolding units of *Pseudomonas aeruginosa* cytochrome c_{551}. *J. Biol. Inorg. Chem. 13*, 837−845.
(29) Duncan, M. G., Williams, M. D., and Bowler, B. E. (2009) Compressing the free energy range of substructure stabilities in iso-1-cytochrome *c*. *Protein Sci. 18*, 1155−1164.
(30) Hoang, L., Maity, H., Krishna, M. M., Lin, Y., and Englander, S. W. (2003) Folding units govern the cytochrome *c* alkaline transition. *J. Mol. Biol. 331*, 37−43.
(31) Nelson, C. J., and Bowler, B. E. (2000) pH dependence of formation of a partially unfolded state of a Lys 73 → His variant of iso-1-cytochrome *c*: Implications for the alkaline conformational transition of cytochrome *c*. *Biochemistry 39*, 13584−13594.
(32) Kristinsson, R., and Bowler, B. E. (2005) Communication of stabilizing energy between substructures of a protein. *Biochemistry 44*, 2349−2359.
(33) Wandschneider, E., Hammack, B. N., and Bowler, B. E. (2003) Evaluation of cooperative interactions between substructures of iso-1-cytochrome *c* using double mutant cycles. *Biochemistry 42*, 10659−10666.
(34) Redzic, J. S., and Bowler, B. E. (2005) Role of hydrogen bond networks and dynamics in positive and negative cooperative stabilization of a protein. *Biochemistry 44*, 2900−2908.
(35) Godbole, S., Hammack, B., and Bowler, B. E. (2000) Measuring denatured state energetics: Deviations from random coil behavior and implications for the folding of iso-1-cytochrome *c*. *J. Mol. Biol. 296*, 217−228.
(36) Hammack, B. N., Smith, C. R., and Bowler, B. E. (2001) Denatured state thermodynamics: Residual structure, chain stiffness and scaling factors. *J. Mol. Biol. 311*, 1091−1104.
(37) Cohen, J. S., and Hayes, M. B. (1974) Nuclear magnetic resonance titration curves of histidine ring protons. *J. Biol. Chem. 249*, 5472−5477.
(38) Pielak, G. J., Auld, D. S., Betz, S. F., Hilgen-Willis, S. E., and Garcia, L. L. (1996) Nuclear magnetic resonance studies of class I cytochromes *c*. In *Cytochrome c: A Multidisciplinary Approach* (Scott, R. A., and Mauk, A. G., Eds.) pp 203−284, University Science Books, Sausalito, CA.
(39) Hartshorn, R. T., and Moore, G. R. (1989) A denaturation-induced proton-uptake study of horse ferricytochrome *c*. *Biochem. J. 258*, 595−598.
(40) Moore, G. R. (1983) Control of redox properties of cytochrome *c* by special electrostatic interactions. *FEBS Lett. 161*, 171−175.
(41) Hammack, B., Godbole, S., and Bowler, B. E. (1998) Cytochrome *c* folding traps are not due solely to histidine-heme ligation: Direct demonstration of a role for N-terminal amino group-heme ligation. *J. Mol. Biol. 275*, 719−724.
(42) Bowler, B. E., Dong, A., and Caughey, W. S. (1994) Characterization of the guanidine hydrochloride-denatured state of iso-1-cytochrome *c* by infrared spectroscopy. *Biochemistry 33*, 2402−2408.
(43) Bandi, S., Baddam, S., and Bowler, B. E. (2007) Alkaline conformational transition and gated electron transfer with a Lys 79 → His variant of iso-1-cytochrome *c*. *Biochemistry 46*, 10643−10654.
(44) Margoliash, E., and Frohwirt, N. (1959) Spectrum of horse-heart cytochrome *c*. *Biochem. J. 71*, 570−572.
(45) Baddam, S., and Bowler, B. E. (2006) Mutation of asparagine 52 to glycine promotes the alkaline form of iso-1-cytochrome *c* and causes loss of cooperativity in acid unfolding. *Biochemistry 45*, 4611−4619.
(46) Rao, K. S., Albro, M., Dwyer, T. M., and Frerman, F. E. (2006) Kinetic mechanism of glutaryl-CoA dehydrogenase. *Biochemistry 45*, 15853−15861.
(47) Matsubara, T., and Ford, P. C. (1978) Photochemistry of ruthenium(II)-saturated amine complexes $Ru(NH_3)_6^{2+}$, $Ru(NH_3)_5H_2O^{2+}$, and $Ru(en)_3^{2+}$ in aqueous solution. *Inorg. Chem. 17*, 1747−1752.
(48) Meyer, T. J., and Taube, H. (1968) Electron transfer reactions of ruthenium ammines. *Inorg. Chem. 7*, 2369−2370.
(49) Qin, W., Sanishvili, R., Plotkin, B., Schejter, A., and Margoliash, E. (1995) The role of histidines 26 and 33 in the structural stabilization of cytochrome *c*. *Biochim. Biophys. Acta 1252*, 87−94.
(50) Berghuis, A. M., and Brayer, G. D. (1992) Oxidation state-dependent conformational changes in cytochrome *c*. *J. Mol. Biol. 223*, 959−976.
(51) Eaton, W. A., and Hochstrasser, R. M. (1967) Electronic spectrum of single crystals of ferricytochrome *c*. *J. Chem. Phys. 46*, 2533−2539.
(52) Dragomir, I., Hagarman, A., Wallace, C., and Schweitzer-Stenner, R. (2007) Optical band splitting in cytochrome *c* at room temperature probed by visible electronic circular dichroism spectroscopy. *Biophys. J. 92*, 989−998.
(53) Battistuzzi, G., Borsari, M., De Rienzo, F., Di Rocco, G., Ranieri, A., and Sola, M. (2007) Free energy of transition for the individual alkaline conformers of yeast iso-1-cytochrome *c*. *Biochemistry 46*, 1694−1702.
(54) Myers, J. K., Pace, C. N., and Scholtz, J. M. (1995) Denaturant *m* values and heat capacity changes: Relation to changes in accessible surface areas of protein unfolding. *Protein Sci. 4*, 2138−2148.
(55) Schellman, J. A. (1978) Solvent denaturation. *Biopolymers 17*, 1305−1322.
(56) Betz, S. F., and Pielak, G. J. (1992) Introduction of a disulfide bond into cytochrome *c* stabilizes a compact denatured state. *Biochemistry 31*, 12337−12344.
(57) Pearce, L. L., Gartner, A. L., Smith, M., and Mauk, A. G. (1989) Mutation-induced perturbation of the cytochrome *c* alkaline transition. *Biochemistry 28*, 3152−3156.
(58) Wherland, S., and Gray, H. B. (1977) Electron transfer mechanisms employed by metalloproteins. In *Biological Aspects of*

Inorganic Chemistry (Addison, A. W., Cullen, W. R., Dolphin, D., and James, B. R., Eds.) pp 289−368, Wiley-Interscience, New York.
(59) Barker, P. D., and Mauk, A. G. (1992) pH-linked conformational regulation of a metalloprotein oxidation-reduction equilibrium: Electrochemical analysis of the alkaline form of cytochrome *c*. *J. Am. Chem. Soc. 114*, 3619−3624.
(60) Feinberg, B. A., Liu, X., Ryan, M. D., Schejter, A., Zhang, C. Y., and Margoliash, E. (1998) Direct voltammetric observation of redox driven changes in axial coordination and intramolecular rearrangement of the phenylalanine-82-histidine variant of yeast iso-1-cytochrome *c*. *Biochemistry 37*, 13091−13101.
(61) Raphael, A. L., and Gray, H. B. (1989) Axial ligand replacement in horse heart cytochrome *c* by semisynthesis. *Proteins: Struct., Funct., Genet. 6*, 338−340.
(62) Raphael, A. L., and Gray, H. B. (1991) Semisynthesis of axial-ligand (position-80) mutants of cytochrome *c*. *J. Am. Chem. Soc. 113*, 1038−1040.
(63) Baddam, S., and Bowler, B. E. (2006) Tuning the rate and pH accessibility of a conformational electron transfer gate. *Inorg. Chem. 45*, 6338−6346.
(64) Baddam, S., and Bowler, B. E. (2005) Conformationally gated electron transfer in iso-1-cytochrome *c*: Engineering the rate of a conformational switch. *J. Am. Chem. Soc. 127*, 9702−9703.
(65) Greenwood, C., and Palmer, G. (1965) Evidence for the existence of two functionally distinct forms of cytochrome *c* monomer at alkaline pH. *J. Biol. Chem. 240*, 3660−3663.
(66) Wilson, M. T., and Greenwood, C. (1971) Studies on ferricytochrome *c*. 2. A correlation between reducibility and the possession of the 695 nm absorption band of ferricytochrome *c*. *Eur. J. Biochem. 22*, 11−18.
(67) Hodges, H. L., Holwerda, R. A., and Gray, H. B. (1974) Kinetic studies of reduction of ferricytochrome *c* by $Fe(EDTA)^{2-}$. *J. Am. Chem. Soc. 96*, 3132−3137.
(68) Bowler, B. E., Raphael, A. L., and Gray, H. B. (1990) Long-range electron-transfer in donor (spacer) acceptor molecules and proteins. *Prog. Inorg. Chem. 38*, 259−322.
(69) Cusanovich, M. A., and Tollin, G. (1996) Kinetics of electron transfer of *c*-type cytochromes with small reagents. In *Cytochrome c: A Multidisciplinary Approach* (Scott, R. A., and Mauk, A. G., Eds.) pp 489−513, University Science Books, Sausalito, CA.
(70) Meagher, N. E., Juntunen, K. L., Salhi, C. A., Ochrymowycz, L. A., and Rorabacher, D. B. (1992) Gated electron-transfer behavior in copper(II/I) systems. Comparison of the kinetics for homogeneous cross reactions, NMR self-exchange relaxation, and electrochemical data for a copper macrocyclic tetrathioether complex in aqueous solution. *J. Am. Chem. Soc. 114*, 10411−10420.
(71) Rorabacher, D. B. (2004) Electron transfer by copper centers. *Chem. Rev. 104*, 651−697.
(72) Wijetunge, P., Kulatilleke, C. P., Dressel, L. T., Heeg, M. J., Ochrymowycz, L. A., and Rorabacher, D. B. (2000) Effect of conformational constraints on gated electron-transfer kinetics. 3. Copper(II/I) complexes with cis- and trans-cyclopentanediyl-1,4,8,11-tetrathiacyclotetradecane. *Inorg. Chem. 39*, 2897−2905.
(73) Davidson, V. L. (2008) Protein control of true, gated, and coupled electron transfer reactions. *Acc. Chem. Res. 41*, 730−738.
(74) Davidson, V. L. (2000) What controls the rates of interprotein electron-transfer reactions. *Acc. Chem. Res. 33*, 87−93.
(75) Espenson, J. H. (1995) *Chemical Kinetics and Reaction Mechanisms*, 2nd ed., McGraw-Hill, Inc., New York.
(76) Drake, P. L., Hartshorn, R. T., McGinnis, J., and Sykes, A. G. (1989) pH-dependence of rate constants for reactions of cytochrome *c* with inorganic redox partners and mechanistic implications. *Inorg. Chem. 28*, 1361−1366.
(77) Nocera, D. G., Winkler, J. R., Yocom, K. M., Bordignon, E., and Gray, H. B. (1984) Kinetics of intramolecular electron transfer from Ru^{II} to Fe^{III} in ruthenium-modified cytochrome *c*. *J. Am. Chem. Soc. 106*, 5145−5150.
(78) D'Amico, S., Marx, J. C., Gerday, C., and Feller, G. (2003) Activity-stability relationships in extremophilic enzymes. *J. Biol. Chem. 278*, 7891−7896.
(79) Hong, X., and Dixon, D. W. (1989) NMR study of the alkaline isomerization of ferricytochrome *c*. *FEBS Lett. 246*, 105−108.
(80) Rosell, F. I., Harris, T. R., Hildebrand, D. P., Döpner, S., Hildebrandt, P., and Mauk, A. G. (2000) Characterization of an alkaline transition intermediate stabilized in the Phe82Trp variant of yeast iso-1-cytochrome *c*. *Biochemistry 39*, 9047−9054.
(81) Godbole, S., Dong, A., Garbin, K., and Bowler, B. E. (1997) A lysine 73 → histidine variant of yeast iso-1-cytochrome *c*: Evidence for a native-like intermediate in the unfolding pathway and implications for *m* value effects. *Biochemistry 36*, 119−126.